

## Strain-Controlled Tensile Deformation Behavior and Relaxation Properties of Isotactic Poly(1-butene) and Its Ethylene Copolymers

Mahmoud Al-Hussein, Gert Strobl\*

Physikalisches Institut, Albert-Ludwigs-Universität, Hermann-Herder-Str. 3, 79104 Freiburg, Germany

E-mail: gert.strobl@physik.uni-freiburg.de

**Summary:** The tensile deformation behaviour of poly(1-butene) and two of its ethylene copolymers was studied at room temperature. This was done by investigating true stress-strain curves at constant strain rates, elastic recovery and stress relaxation properties and in-situ WAXS patterns during the deformation process. As for a series of semicrystalline polymers in previous studies, a strain-controlled deformation behaviour was found. The differential compliance, the recovery properties and the stress relaxation curves changed simultaneously at well-defined points. The strains at which these points occurred along the true stress-strain remained constant for the different samples despite their different percentage crystallinities. The well-defined way in which the different samples respond to external stresses complies with the granular substructure of the crystalline lamellae in a semicrystalline polymer.

**Keywords:** deformation; poly(1-butene); relaxation; recovery; yielding

### Introduction

In previous papers we reported on the tensile deformation behavior of several polyethylenes and s-polypropylenes based upon measurements of true stress-strain curves, elastic-recovery properties, and texture changes at different stages of the deformation process. The results<sup>[1-3]</sup> showed that there is a general scheme that governs the behavior. Along the true stress-strain curve, the differential compliance, the recovery properties, and the crystallite texture change simultaneously at well-defined points. The strains at these points are invariant over various crystallinities, strain rates and drawing temperatures. In contrast to this, the corresponding stresses vary considerably.

In a subsequent paper, we reported on the tensile deformation of a set of poly(1-butene)-based samples with different crystallinities. Poly(1-butene) (P1B) is renowned for its good creep resistance and the retaining of its mechanical properties at elevated temperatures. The mechanical tests were now further expanded, by the inclusion of stress relaxation measurements.

**Experimental**

*Sample characteristics and preparation*

Three different P1B-based samples (provided by Basell, Louvain-La-Neuve, Belgium), were used in this study. Their characteristics are shown in Table 1.

Table 1. Sample Characteristics of P1B

sample	grade	ethylene %	$T_m/^{\circ}\text{C}$	crystallinity %
A	PB0300	0	123	47
B	PB8220	6	119	37
C	PB010	>6	108	16

Compression-moulded sheets were prepared from the different samples. After cooling, the sheets were stored at room temperature for at least 40 days to allow the samples to transform into their stable form I. Then dog-bone-shaped specimens of 6.5 x 4 mm were cut from the sheets for testing.

*True stress-strain curves*

True stress-strain curves at a constant Hencky strain rate were obtained using a video-controlled tensile testing apparatus. It employs a video camera connected to a computer to control the deformation by regulating the cross-head speed in a way that keeps the Hencky strain rate at a constant value.

### ***Recovery and stress relaxation***

The same apparatus was also used to investigate the elastic recovery properties at different stages of the deformation process. This was done by carrying out a step-cycle test. A specimen is stretched first to a predetermined strain,  $\epsilon_{\text{tot}}$ , and then it is brought back to a zero stress. The remaining strain at this point represents the plastic part,  $\epsilon_{\text{pla}}$ , and the difference between the total and plastic strain gives the elastic part,  $\epsilon_{\text{ela}}$ .

The apparatus was also used for the stress relaxation measurements. A test specimen is stretched first to a predetermined strain at a constant strain rate, as explained above. Subsequently, the strain is held constant and the force decay is followed with time. The prior stretching was performed at a constant true strain rate of  $0.005 \text{ s}^{-1}$  for all measurements.

## **Results**

### ***Deformation Behavior***

Figure 1 shows true stress-strain curves obtained at a constant strain rate of  $0.005 \text{ s}^{-1}$  at room temperature for the different samples. None of the samples showed necking down during deformation despite their different crystallinities. The different curves are similar to each other, resembling a rubber-like behavior.

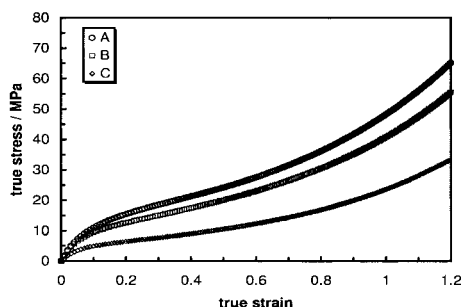


Figure 1. True stress-strain curves obtained at true strain rate of  $0.005 \text{ s}^{-1}$  of samples A, B and C.

Step-cycle tests were used to decompose the imposed strain into elastic and plastic parts that were recoverable and irrecoverable, respectively, on the time scale of the experiment and at room temperature. A representative example of a step-cycle test is given in Figure 2. The total, plastic, and elastic strain was then plotted as a function of the true stress (Figure 3).

As can be seen, at the beginning of the deformation process, both the plastic and elastic strain increased with increasing total strain. This carried on until the total strain reached a certain value, at which the elastic strain assumed a plateau value, and any further increase in the total strain proceeded by only increasing the plastic strain. This occurs at a point, which we refer to as point C. The interesting feature is that the total strain at point C was common for the different samples,  $\epsilon_H \approx 0.7$ .

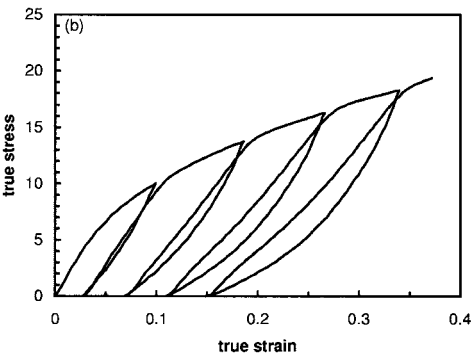


Figure 2. A representative example of the step-cycle test (sample A).

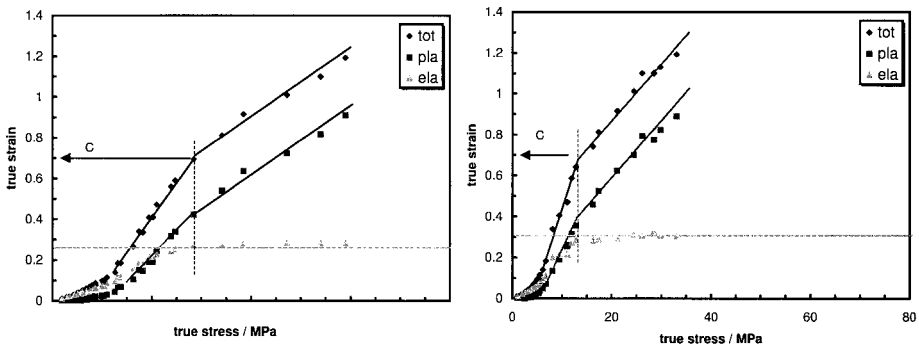


Figure 3. True total and elastic strain at different imposed true stresses for the different samples, A (left) and C (right).

Looking more closely at the low deformation region revealed another two transition points, A and B, which occurred again at the same strains of 0.05 and 0.1, respectively, for all samples. Figure 4 shows typical examples of stress relaxation tests performed at different strains. It can be seen that the stress always decreased and eventually approached a final plateau value. There was no substantial change in the shape of the relaxation curve up to a strain of 0.7. After this strain the amount of stress relaxation increased.

To learn more about a possible cause of this increase we examined the strain rate effect. Figure 5 shows the stress relaxation curves obtained after stretching to a true strain of 1, at three different strain rates. As seen, whilst the plateau value changed only slightly, the initial stress drop showed a strong dependence on the strain rate. Obviously this drop is associated with the cessation of an instantaneous viscous flow component.

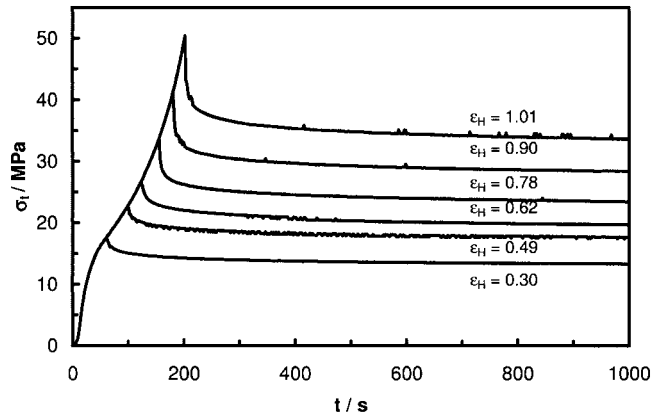


Figure 4. Stress relaxation test at the indicated Hencky strains (sample A).

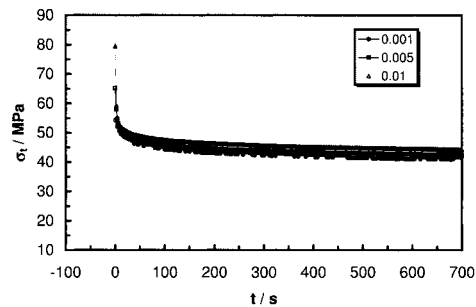


Figure 5. Stress relaxation curves after deformations with the indicated Hencky strain rates to  $\epsilon_H = 1$  (sample A).

It seems that once the deformation stops, this instantaneous flow ceases, and the extra force that was required to keep this flow vanishes. It is evident from Figure 4 that different curves relaxed to different plateau values, which we will refer to as the unrelaxed stress,  $\sigma_{unr}$ . Also notable is the fact that none of the curves relaxed to zero stress even at high strains. In order to quantify the relaxed stress values, we define  $\sigma_{rel}$  as the difference between  $\sigma_0$  and  $\sigma_{unr}$ . Figure 6 shows the

variations of  $\sigma_0$ ,  $\sigma_{unr}$  and  $\sigma_{rel}$  with strain, together with a constant strain rate response. As it can be seen, they all increased with increasing strain.

To investigate whether the relaxation has any effect on the recovery properties we again performed step-cycle tests, but now at the end of the stress relaxation test. Results are shown in Figure 7. The consequence of the stress relaxation was a minor loss in the elastic strain. The position of point C remains unchanged, as shown by Figure 8.

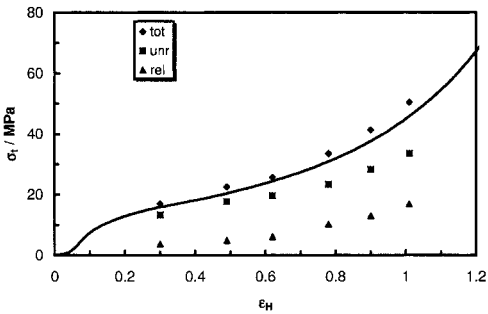


Figure 6. A true stress-strain curve (solid line) together with total, unrelaxed and relaxed stresses at different imposed Hencky strains (sample A).

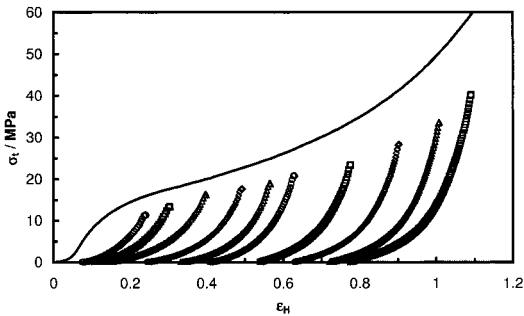


Figure 7. Stress relaxation followed by step-cycle tests at different Hencky strain values (sample A).

# Discussion

Results of the experiments gave us the opportunity to assess the influence of the crystallinity on the deformation behavior for a set of PIB-based samples. As expected, increasing the volume fraction of the crystallites increases the internal friction. This results from inter-and intra-lamellar shear processes. In addition, the different samples showed a common rubber-like deformation behavior. As the deformation proceeded, both the differential compliance and the elastic properties changed at three transition points, A, B, and C, at increasing strain. A Hookean elasticity was exhibited first until point A, where a plastic strain started to occur. Simultaneously, the differential compliance showed a slight increase. This continued up to point B, where another more pronounced increase in the differential compliance took place. Finally, at point C the elastic strain reached a plateau value, and the differential compliance decreased this time. WAXS experiments showed that at point C sharp spots, typical of a fibrillar structure, appeared on the equator.

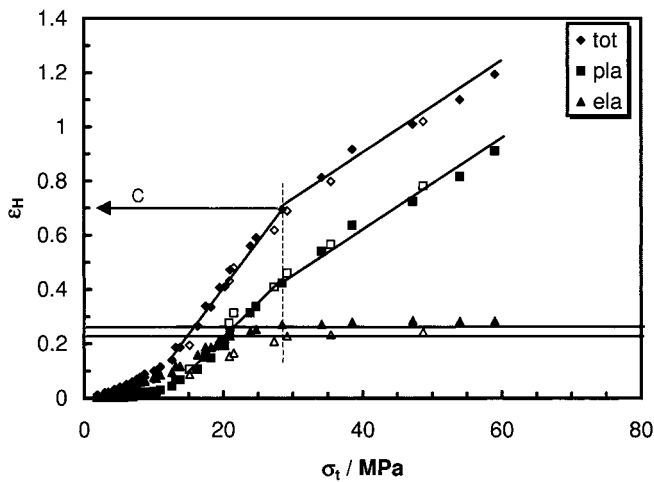


Figure 8. Filled symbols are the total, plastic and elastic strains at different imposed true stresses, as obtained from Figure 7, the open symbols are the same strains as obtained from step-cycle tests without a prior relaxation (Figure 3, left).



Changing the crystallinity of the different samples had no effect on the strain values at which the transition points occurred along a true stress-strain curve. The fact that the strain values of the transition points are unaffected by changing the crystallinity or other factors demonstrates the capability of semicrystalline polymers to accommodate any imposed strain in a rather well defined way. This can only be achieved if there are a sufficient number of internal degrees of freedom available for each semicrystalline polymer by virtue of its structure. This is consistent with recent studies of semicrystalline polymers showing a granular substructure of the crystal lamellae <sup>[4]</sup>. The chain slip processes at the boundary region between the adjacent blocks in a single lamella then provide the extra degrees of freedom needed.

A semicrystalline polymer can be viewed as two interpenetrating networks, a crystalline one intermingled with an entangled amorphous one. Consequently, both of these networks will contribute to any imposed deformation. The extent of each contribution varies during the course of deformation. At low strains, the crystalline network contribution dominates through changing the coupling and invoking some coarse slips of the crystalline blocks (point B). As the strain is increased, the entangled amorphous region becomes increasingly strained. This carries on until a critical strain is reached where the force generated from the entangled fluid regions reaches a critical value that would be able to destroy the crystallites (point C). At this stage the dominant mechanism becomes the disaggregation of the crystallites and apparent recrystallization into fibrill.

Our results also indicate a direct relation between the deformation mechanisms that are active at a certain strain and the subsequent relaxation behaviour. This is demonstrated first by the qualitative change in the shape of the stress relaxation behaviour at point C where an additional viscous force sets in. At low strains and up to the point C, the deformed sample responds mainly by interlamellar shearing and slip processes at the interfaces of the crystalline blocks. Therefore, in order to realize the imposed strain, the blocks have to undergo a continuous readjustment. During this process the majority of the blocks remains intact, but they are away from their equilibrium position. If the crosshead is stopped at any strain in this stage, the blocks pass from their current non-equilibrium states to a new equilibrium state by local movements. This relieves the stress locally and leads to a decrease in the free energy. At point C the initial blocks start to

disintegrate and break away from each other, resulting in a new crystal skeleton with properties different from the original one. The disintegration process contributes to the viscous force and, correspondingly, shows up in the initial decrease in the stress relaxation curves.

[1] R. Hiss, S. Hobeika, C. Lynn and G. Strobl. *Macromolecules* **1998**, 32, 4390.

[2] S. Hobeika, Y. Men and G. Strobl. *Macromolecules* **2000**, 33, 1827.

[3] Y. Men and G. Strobl. *J. Macromol. Sci.* **2001**, 40, 775.

[4] G. Strobl. *Eur. Phys. J. E* **2001**, 3, 165.